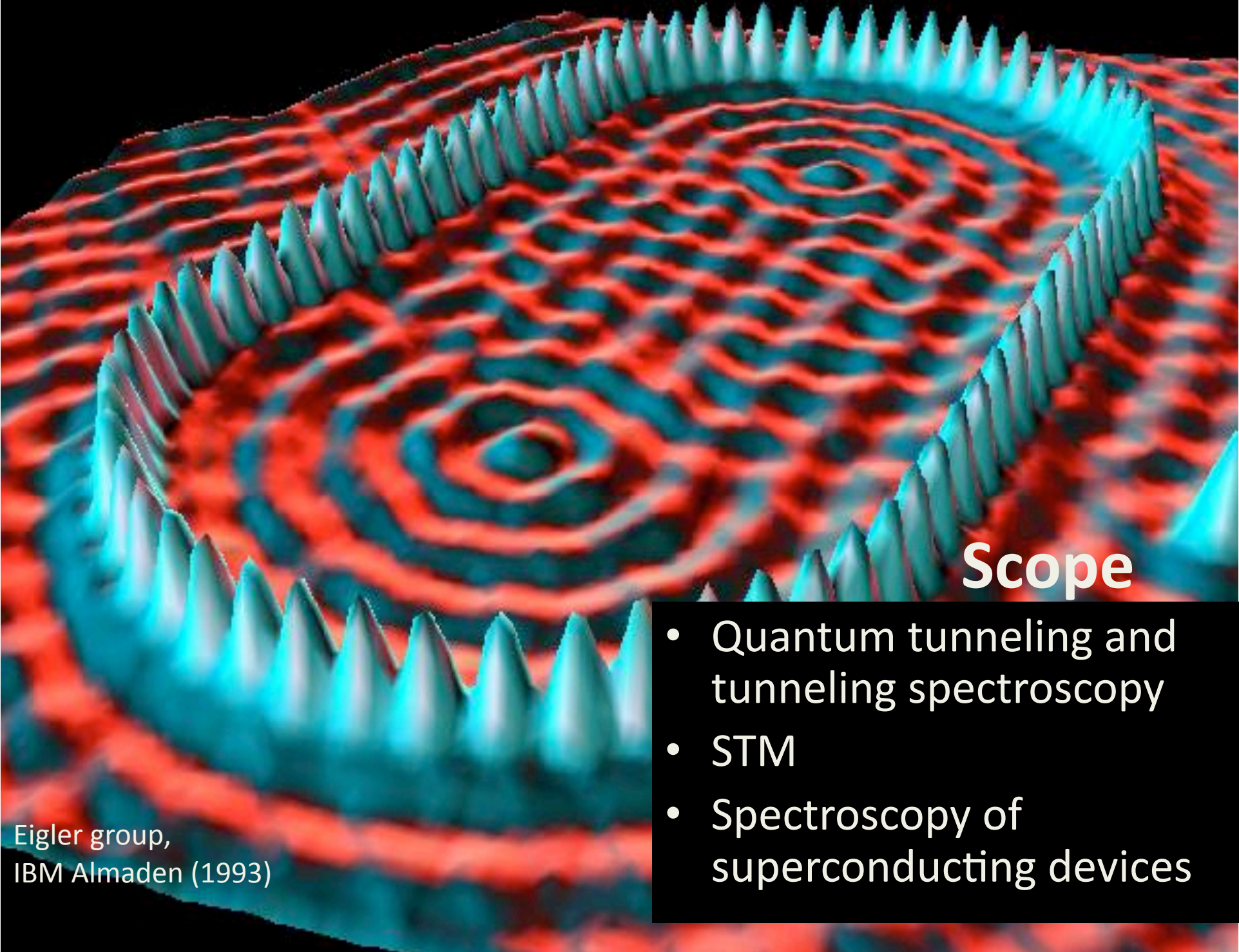


Low temperature scanning tunneling spectroscopy

Clemens.Winkelmann@grenoble.cnrs.fr
Grenoble INP and Institut Néel





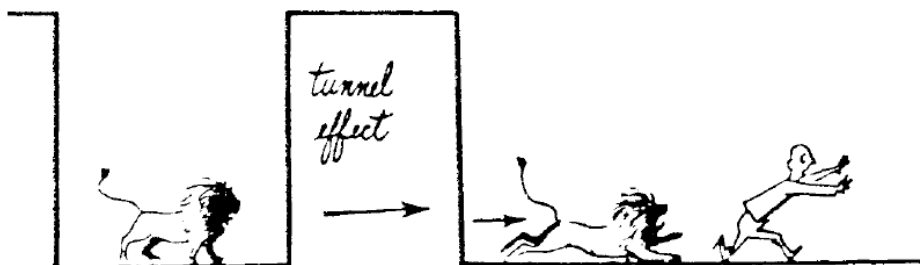
Eigler group,
IBM Almaden (1993)

Scope

- Quantum tunneling and tunneling spectroscopy
- STM
- Spectroscopy of superconducting devices

Quantum tunneling and tunneling spectroscopy

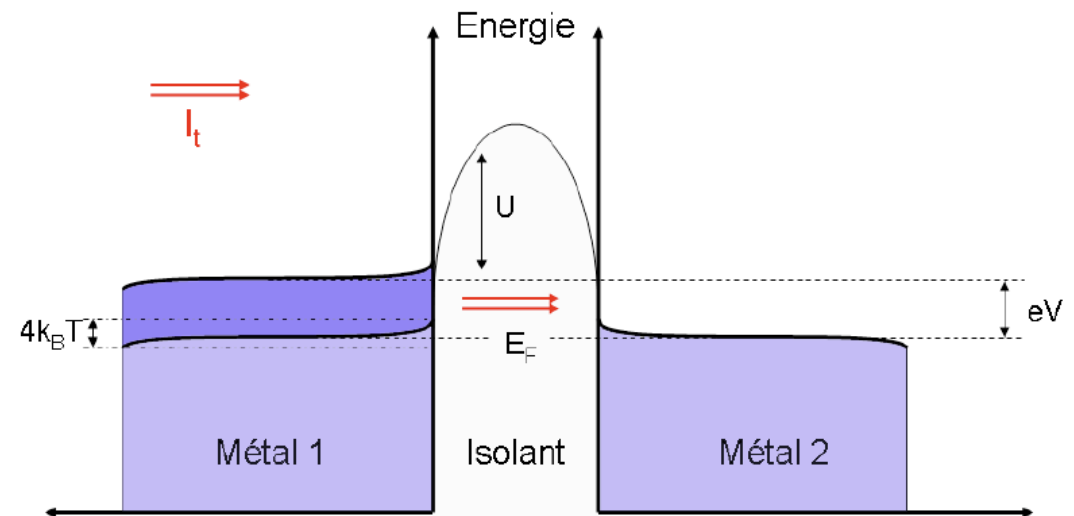
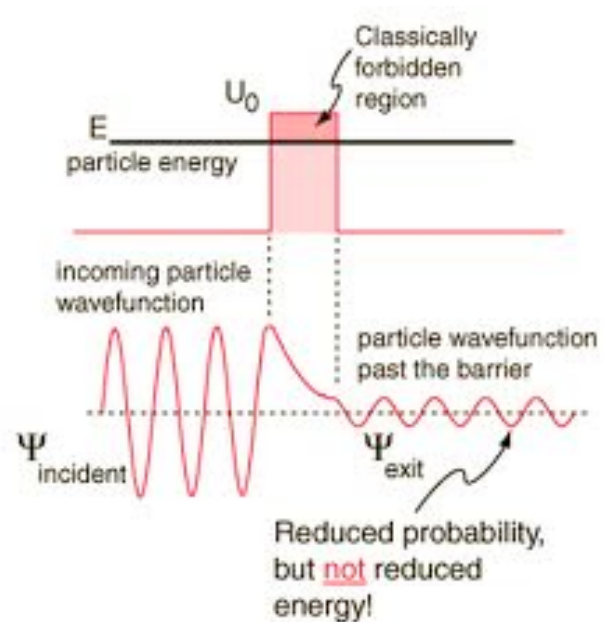
- Local density of states $\rho(r,E)$
- Energy distribution function $f(r,E)$
- Work function W
- Quantum Tunneling



Metal	W (eV)
Li	2.38
Cu	4.4
Au	4.3
Hg	4.52
Al	4.25
W	4.5

Van Vleck, 1979

Quantum tunneling



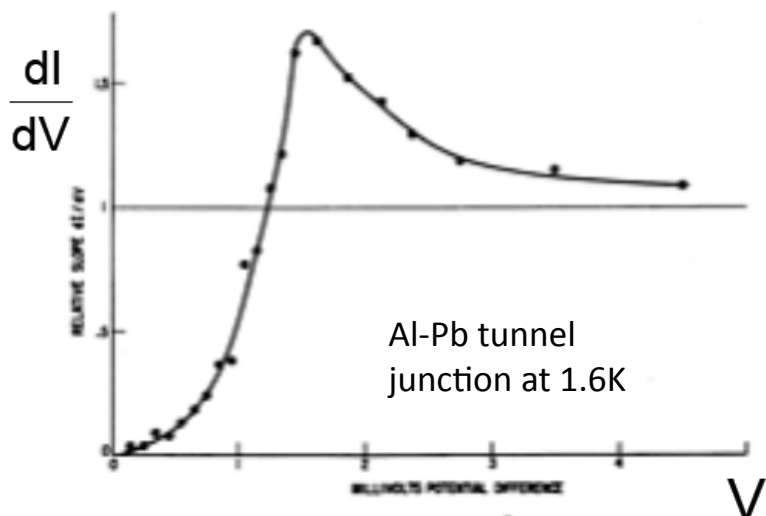
$$M_{\mu\nu} = \frac{\hbar^2}{2m} \int d\vec{S} \cdot (\psi_\mu^* \vec{\nabla} \psi_\nu - \psi_\nu \vec{\nabla} \psi_\mu^*)$$

$$I = \frac{4\pi e}{\hbar} \int_{-\infty}^{+\infty} [f_t(E - eV) - f_s(E)] \times n_t(E - eV) n_s(E) |M|^2 dE$$

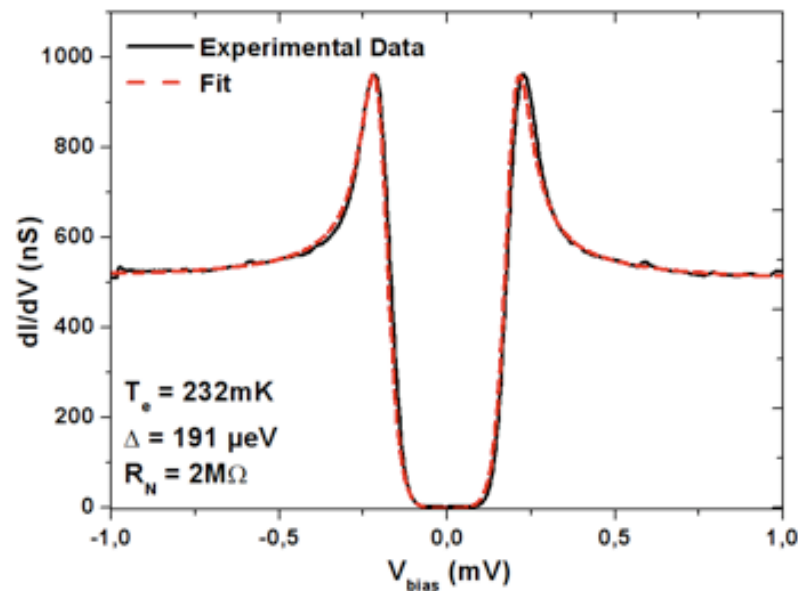
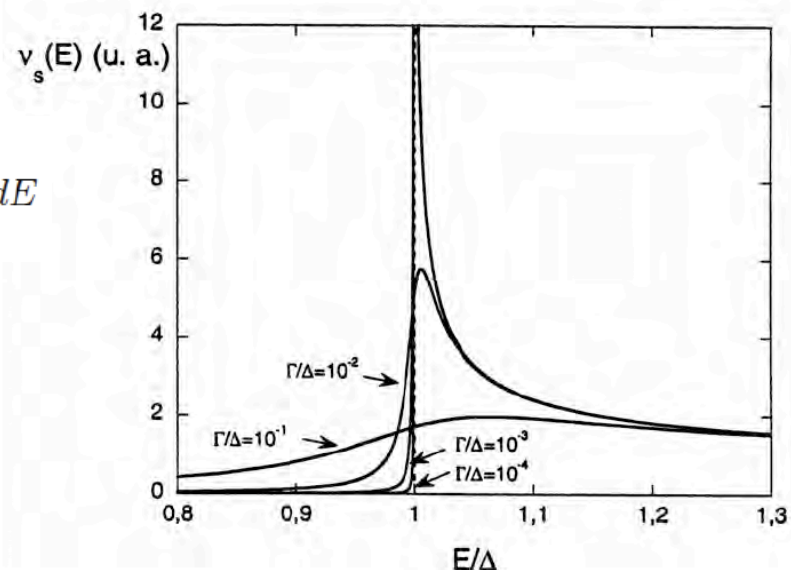
N-I-S tunneling

$$I = \frac{4\pi e}{\hbar} \int_{-\infty}^{+\infty} [f_t(E - eV) - f_s(E)] \times n_t(E - eV) n_s(E) |M|^2 dE$$

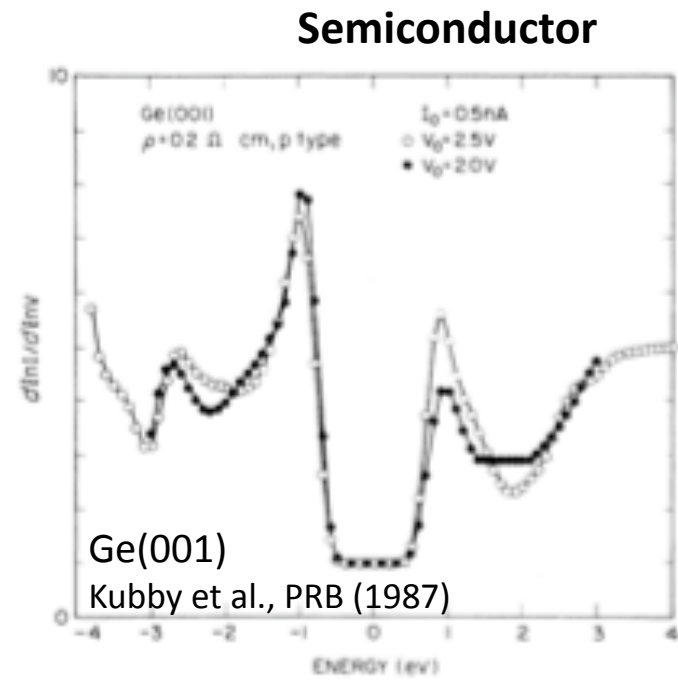
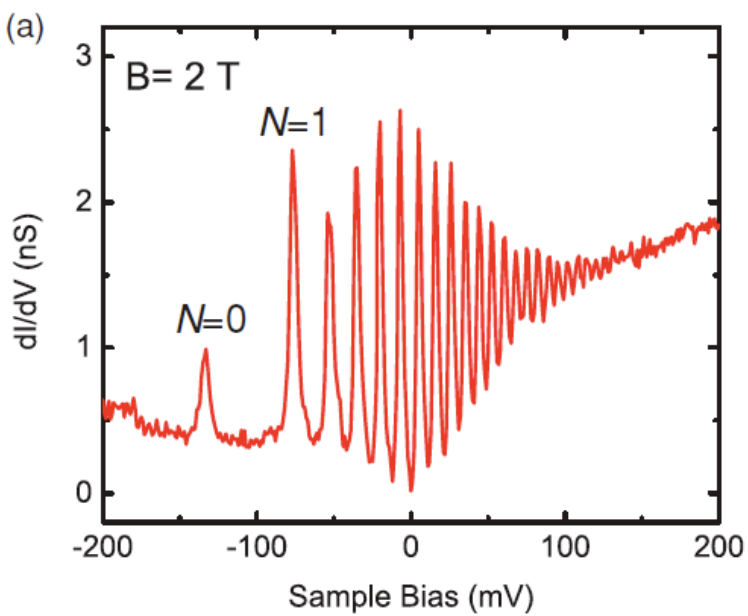
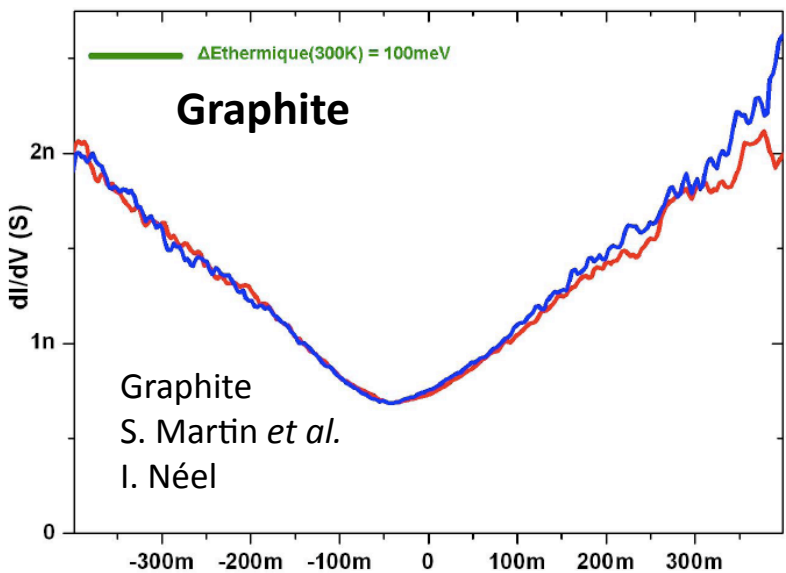
$$\frac{\partial I}{\partial V} \propto \int \frac{\partial f_t}{\partial V}(E - eV) \rho_s(E) dE$$



I. Giaever, Phys. Rev. Lett. 5, 147 (1960)
Nobel prize 1973

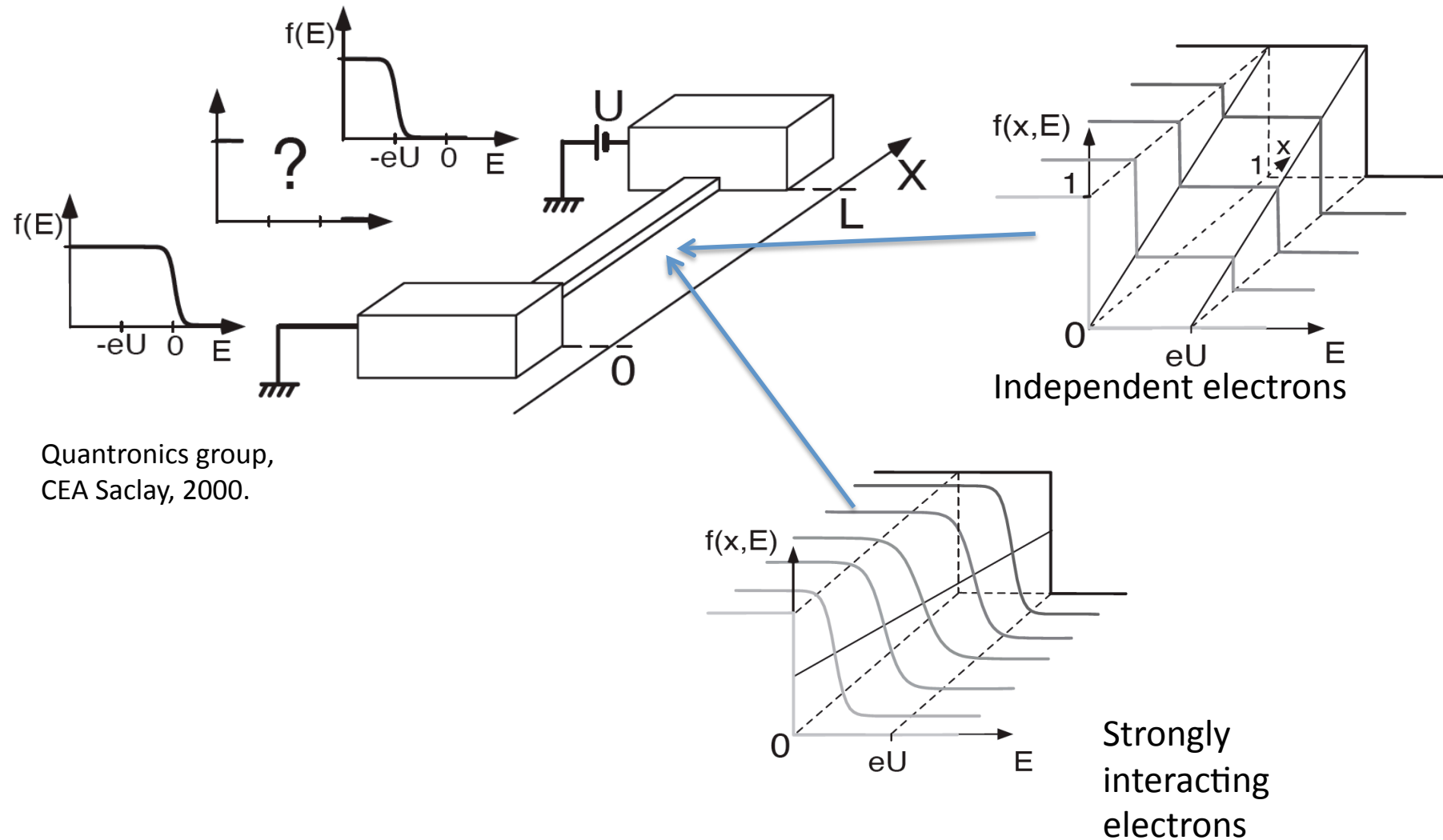


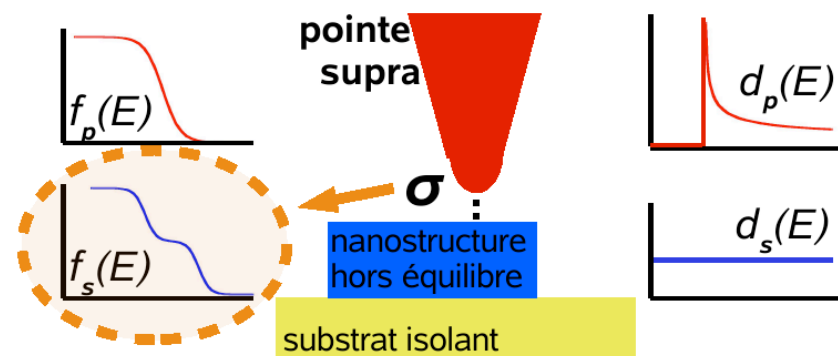
Spectroscopies : examples



Landau levels in graphene
B=2T
Stroscio group, NIST, 2010

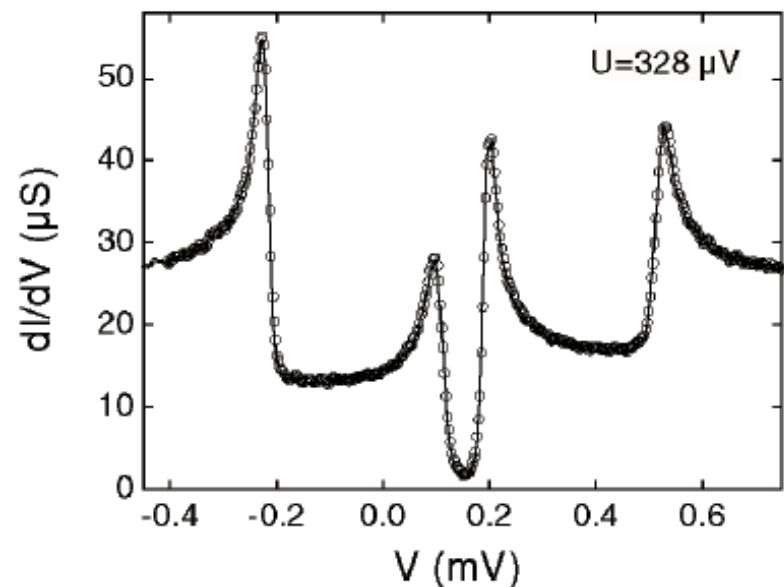
Probing the local energy distribution



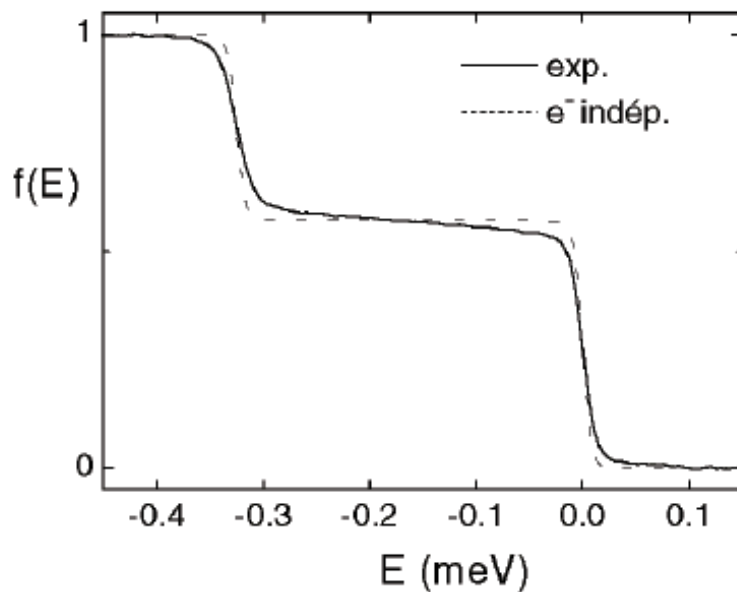


$$\frac{\partial I}{\partial V} \propto \int \frac{\partial f_s}{\partial V} (E - eV) \rho_t(E) dE$$

Quantronics group,
CEA Saclay, 2000.



AgII5



The invention of STM and other near field microscopies

"Tunneling through a controllable vacuum gap", G. Binnig, H. Röhrer, Ch. Gerber and E. Weibel, Appl. Phys. Lett. 40, 178 (1982).

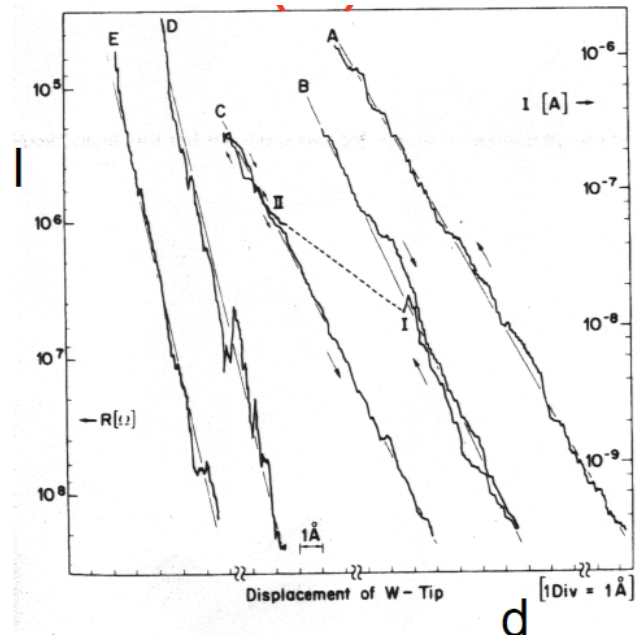
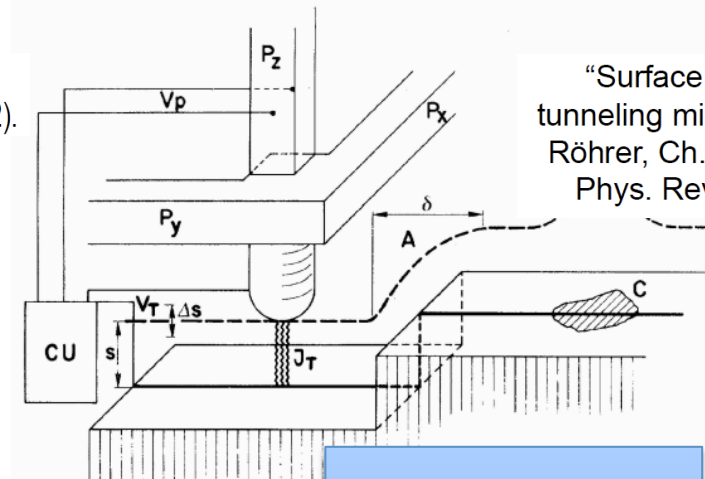
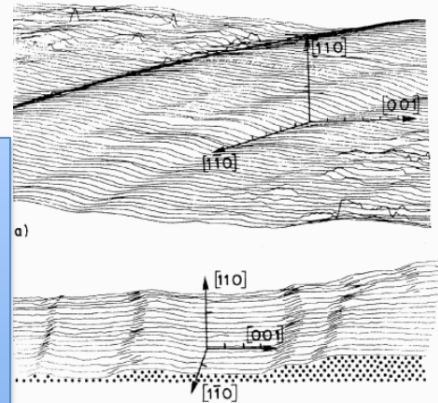
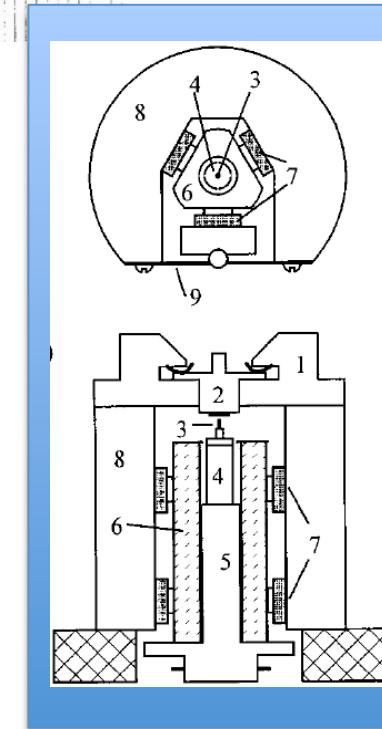


FIG. 2. Tunnel resistance and current vs displacement of Pt plate for different surface conditions as described in the text. The displacement origin is arbitrary for each curve (except for curves B and C with the same origin). The sweep rate was approximately 1 \AA/s . Work functions $\phi = 0.6 \text{ eV}$ and 0.7 eV are derived from curves A, B, and C, respectively. The instability which occurred while scanning B and resulted in a jump from point I to II is attributed to the release of thermal stress in the unit. After this, the tunnel unit remained stable within 0.2 \AA as shown by curve C. After repeated cleaning and in slightly better vacuum, the steepness of curves D and E resulted in $\phi = 3.2 \text{ eV}$.

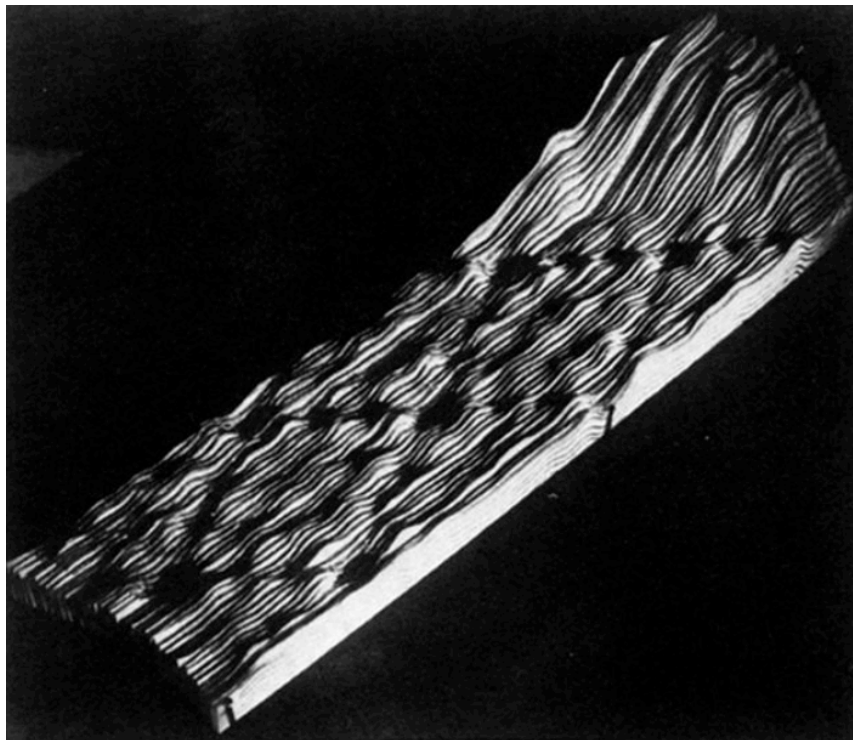


"Surface studies by scanning tunneling microscopy", G. Binnig, H. Röhrer, Ch. Gerber and E. Weibel, Phys. Rev. Lett. 49, 57 (1982).

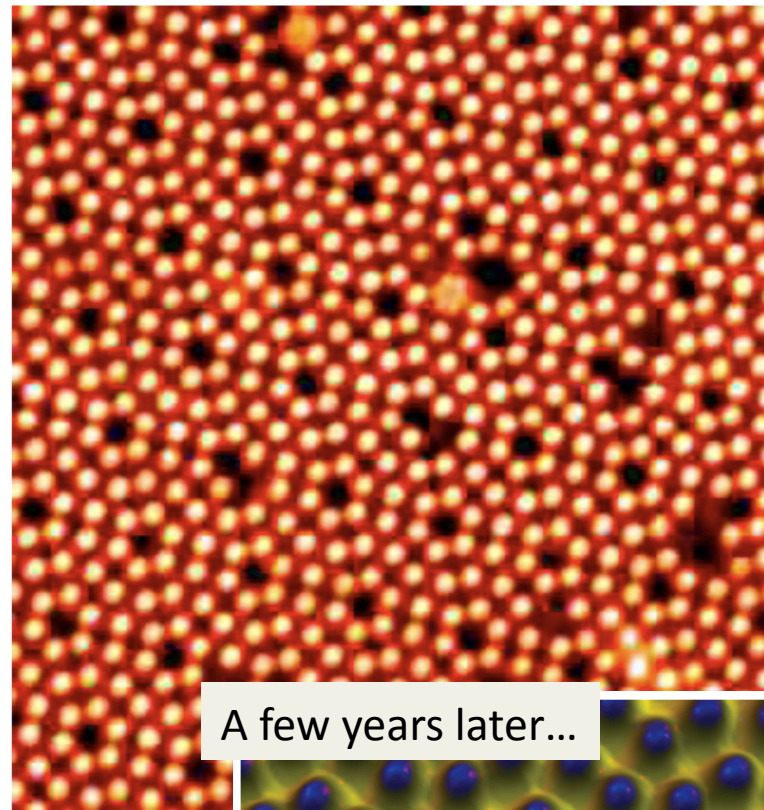


Pan design

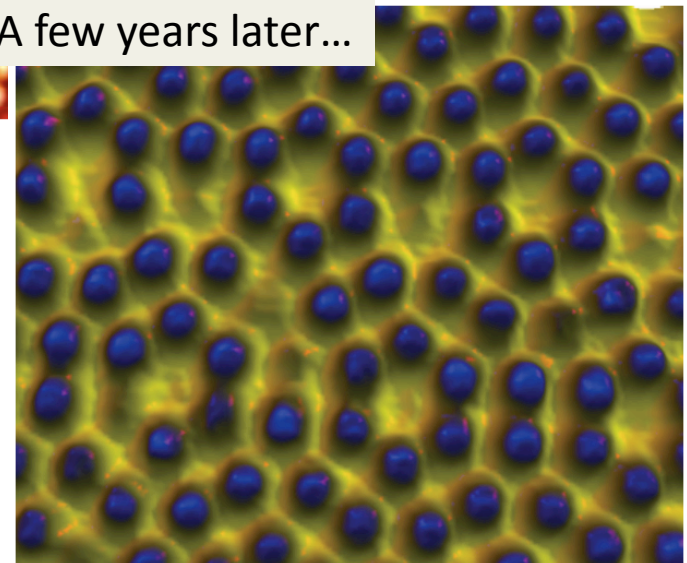
A benchmark in surface science : the 7x7 surface reconstruction of silicon (111)



“7x7 reconstruction on Si (111) resolved in real space”, G. Binnig, H. Röhrer, Ch. Gerber and E. Weibel, Phys. Rev. Lett. 50, 120 (1983).



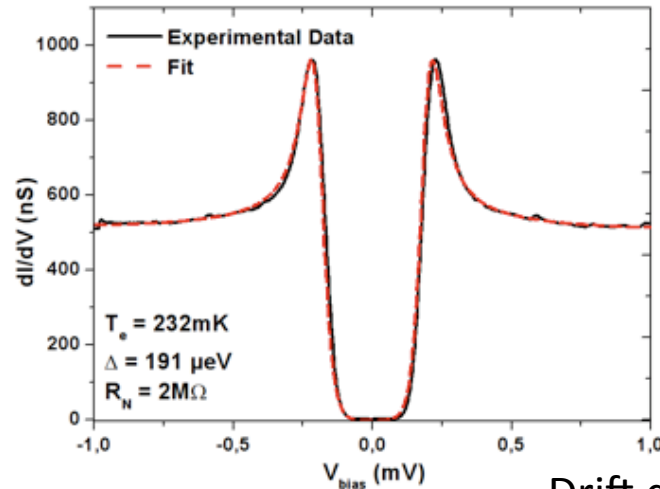
A few years later...



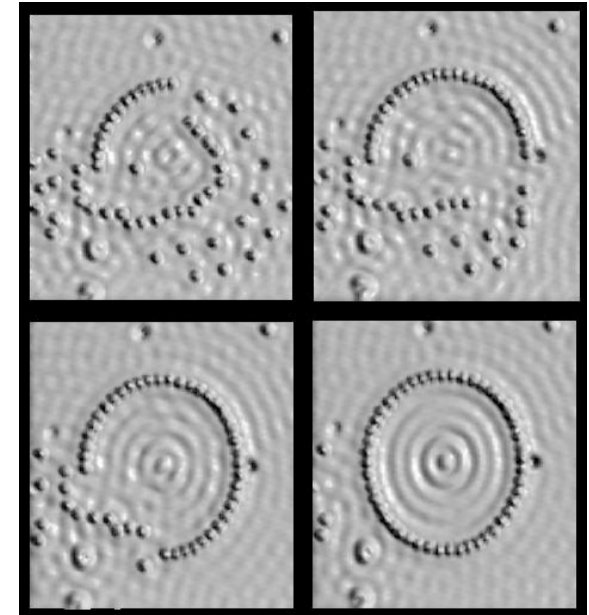
Omicron and Specs websites

Why low temperatures for scanning tunneling microscopy ?

Energy resolution limited by about $4k_B T$



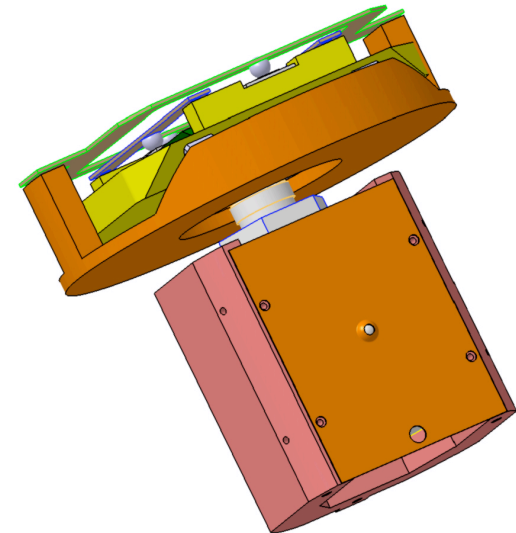
Diffusion of adsorbed atoms/
molecules :
 $T < 10\text{ K}$.

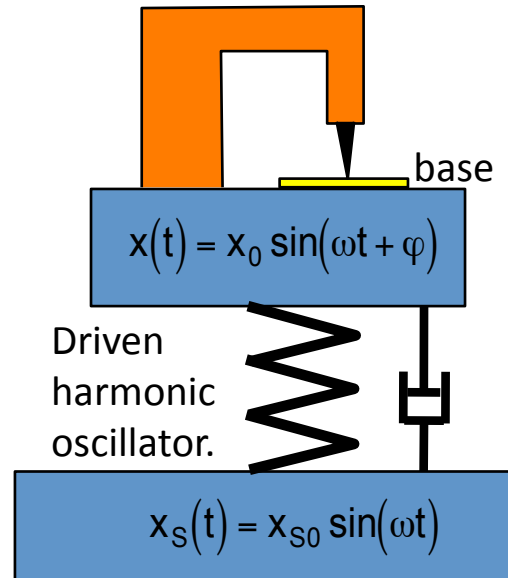


- Drift due to thermal fluctuations
- Increased mechanical rigidity
- Less piezoelectrical hysteresis

But :

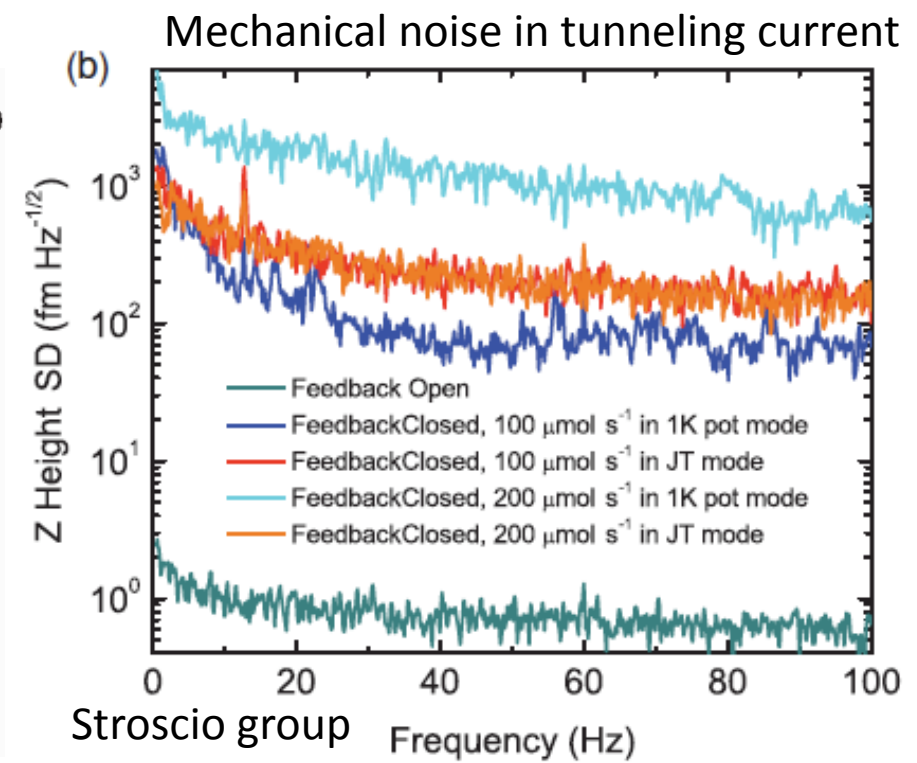
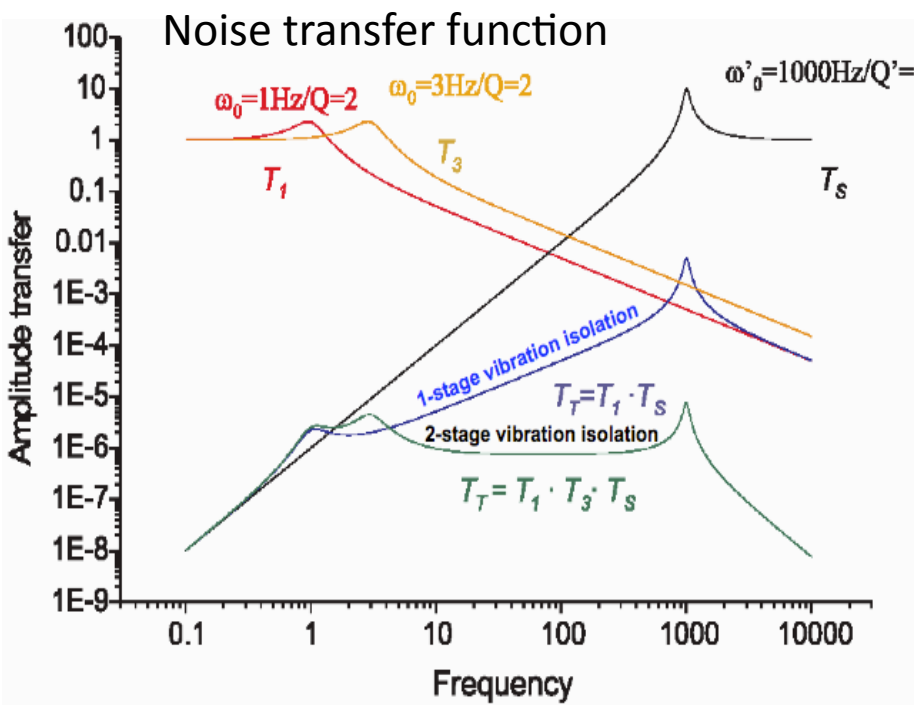
- lower piezoelectric response (factor 5-10),
- thermal anchoring of mechanically mobile parts,
- heat-load and electronic filtering in wiring,
- current amplifier far from sample
- vibrations induced by pumps and helium bath**



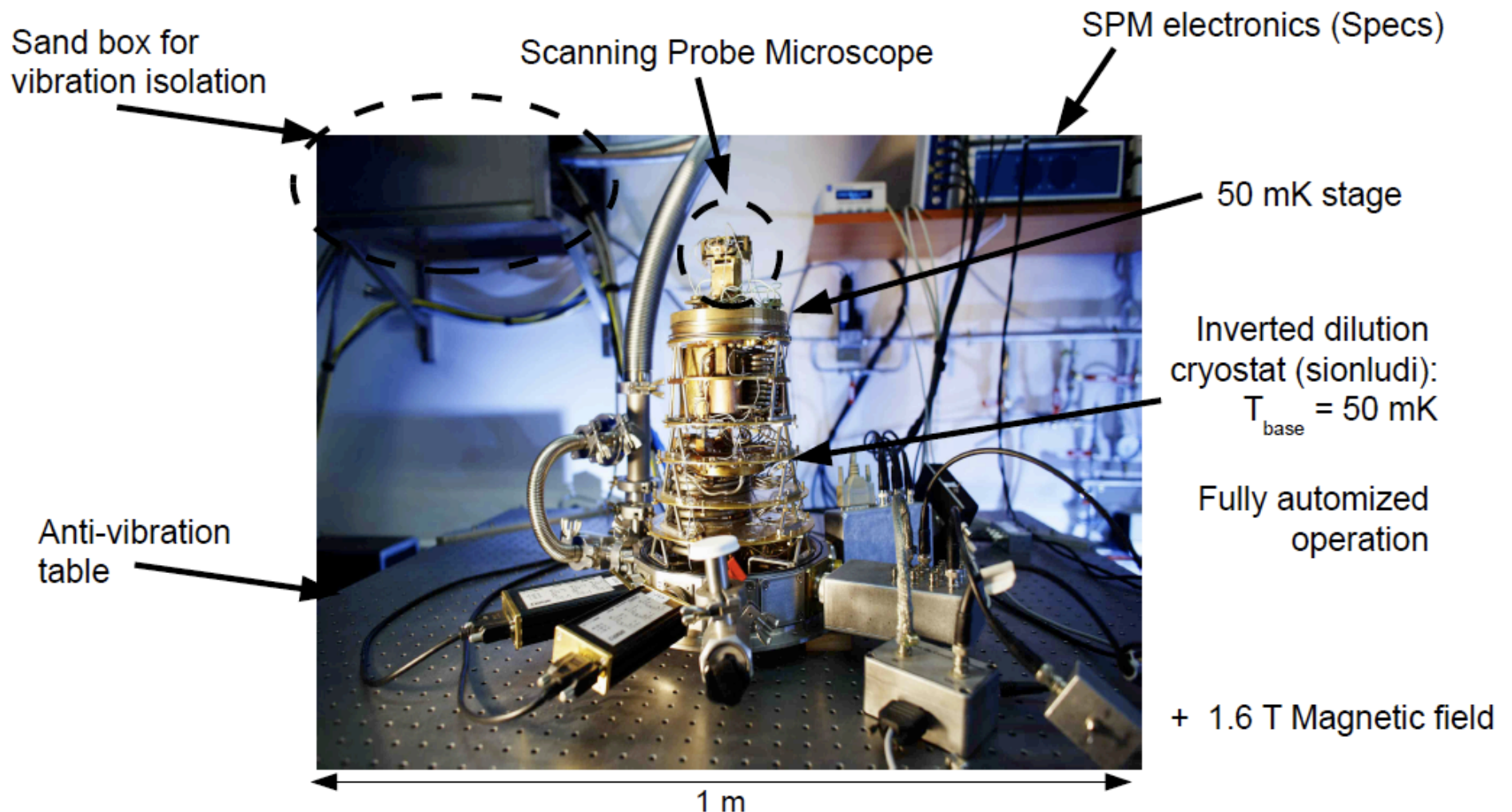


Vibration isolation

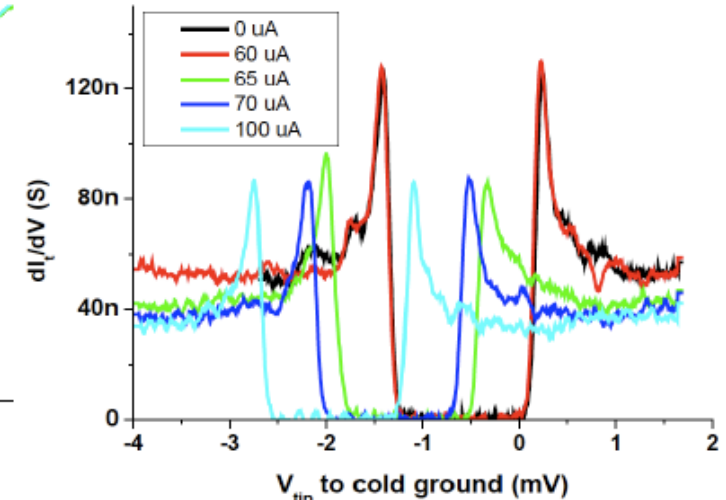
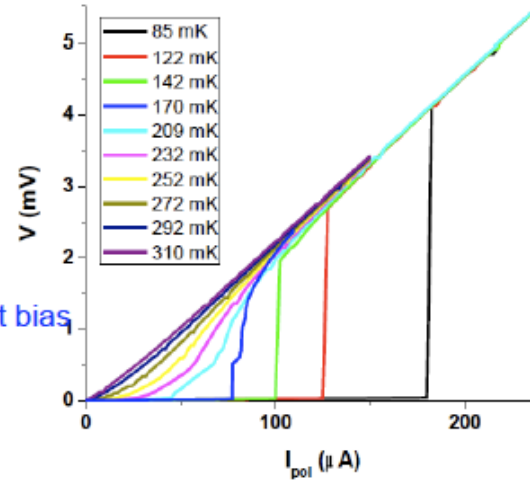
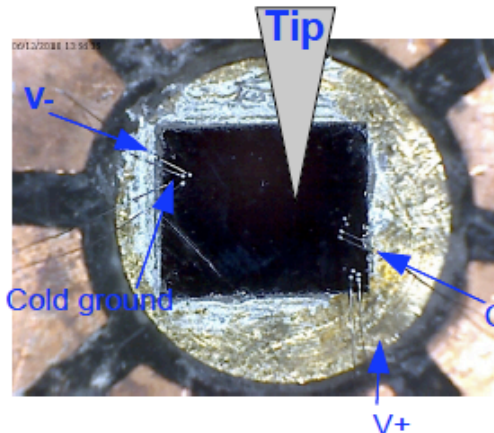
With a 100 nm vibration source at 1 kHz, a 10^{-5} transfer amplitude gives here a 1 pm vibration on the microscope. 10^{-3} gives 100 pm = 1 Å.



Scanning Probe Microscopy at 50 mK



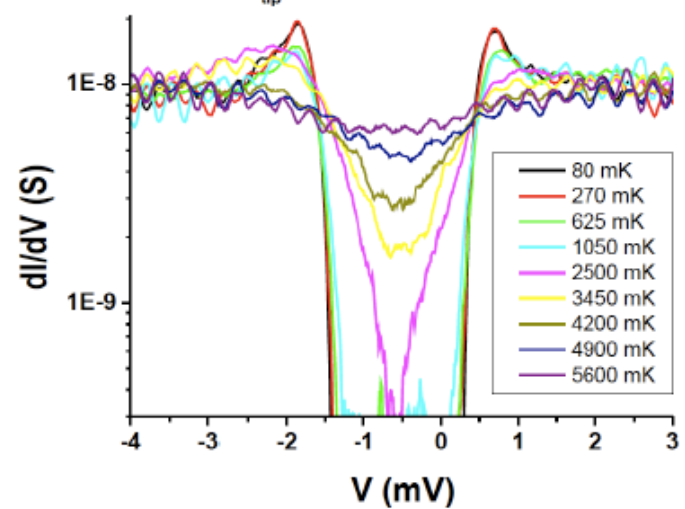
Ge:Ga, an inhomogeneous superconductor ?



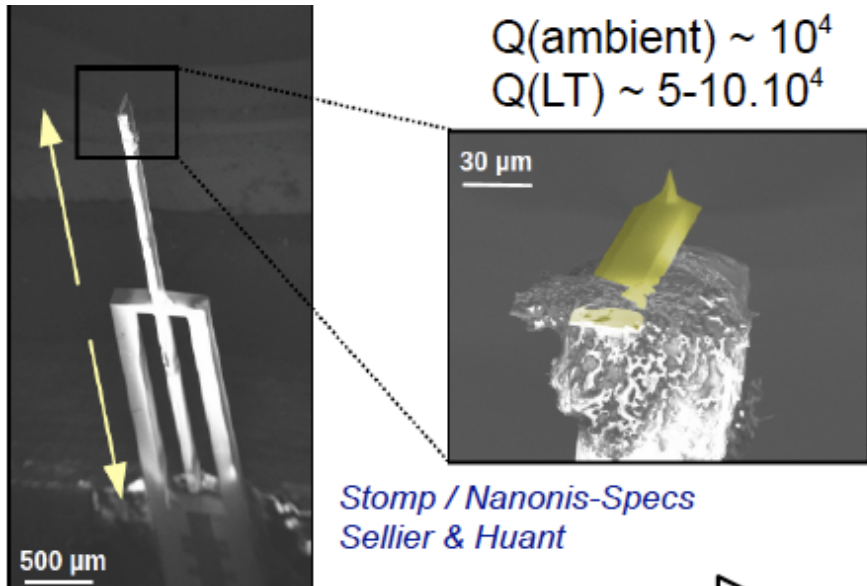
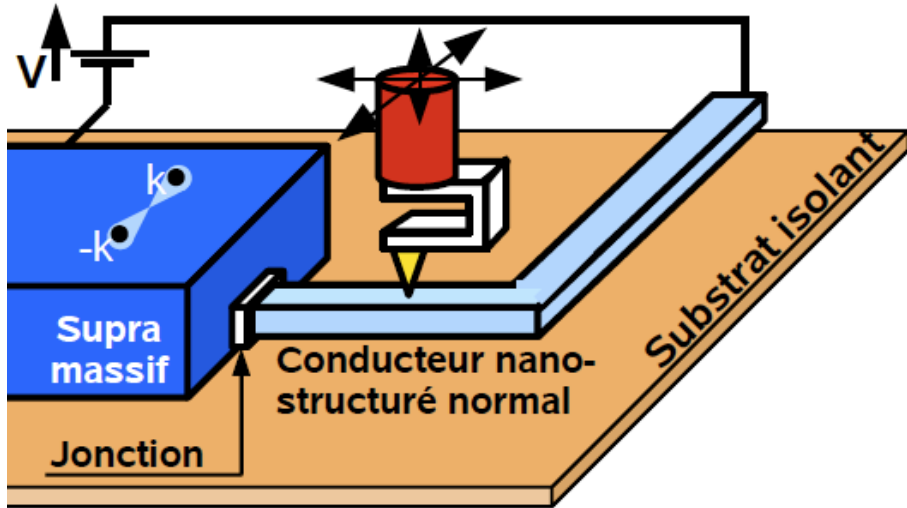
- Superconductivity in heavily Ga doped Ge
Herrmannsdörfer et al., 2009
- Superconducting signature in transport up to < 300mK.
- Tunnel spectroscopy as a function of current bias and temperature : $T_c \sim 6$ K.

Inhomogeneous superconductor, with Josephson-coupled grains ?

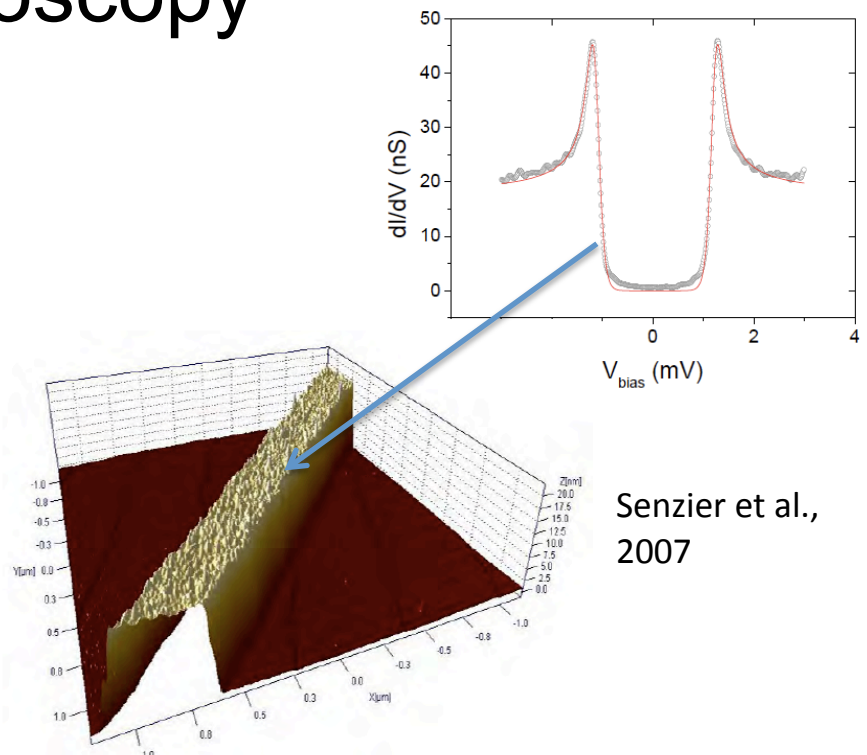
with. V. Heera et al. / Dresden



Spatially resolved spectroscopy in nanodevices

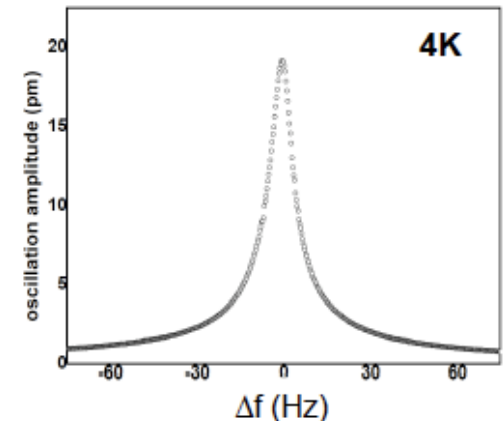


7

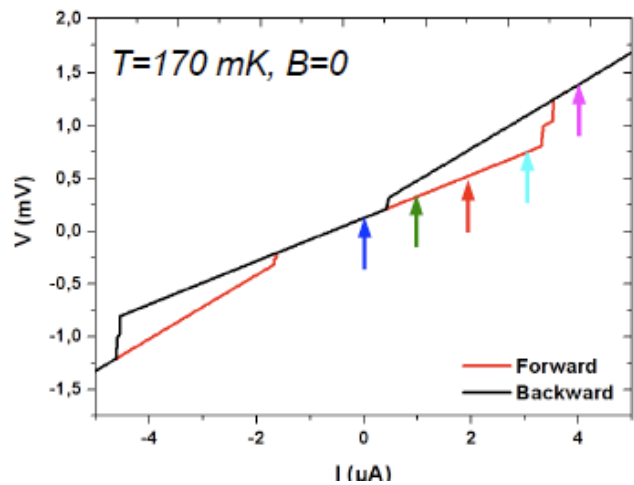
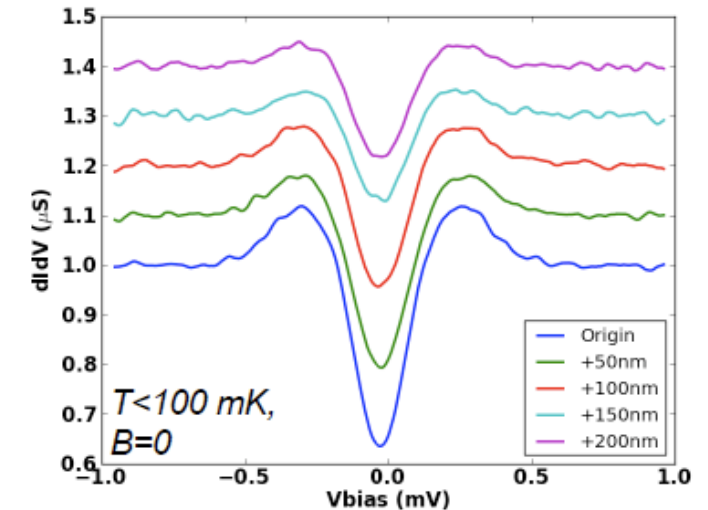
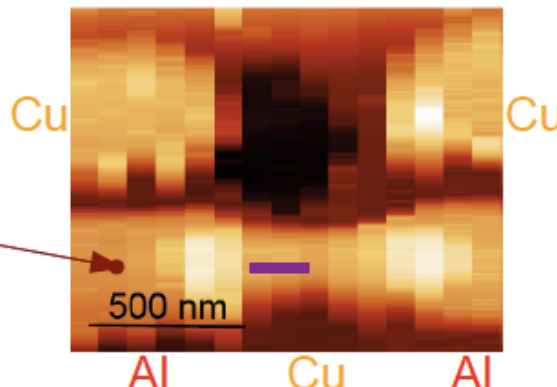
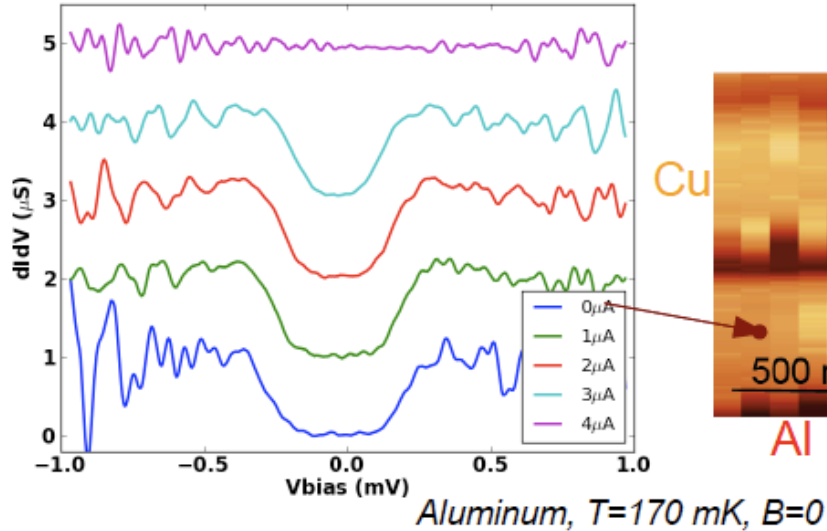


Senzier et al.,
2007

- Tuning fork or length extension resonators :
- no optics
 - fast response
 - high stiffness
 - non-contact mode

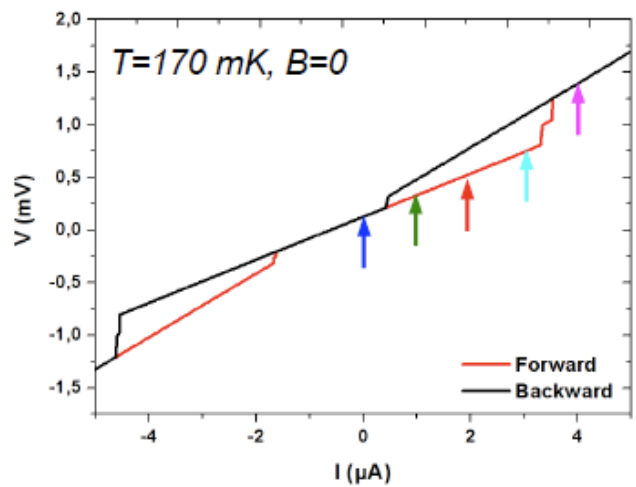
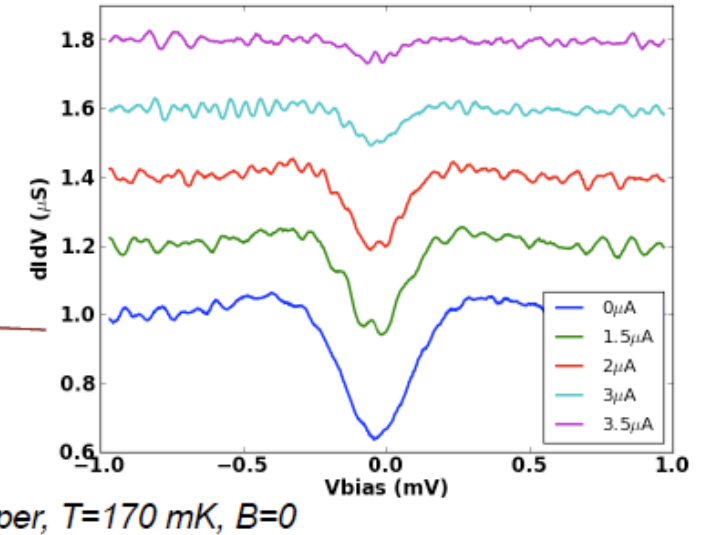
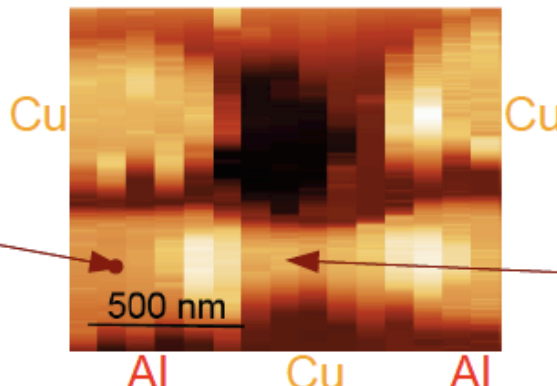
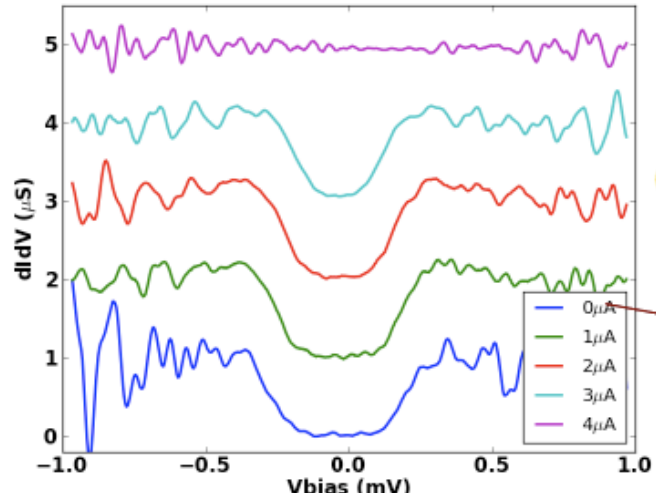


Local spectroscopy in superconducting devices



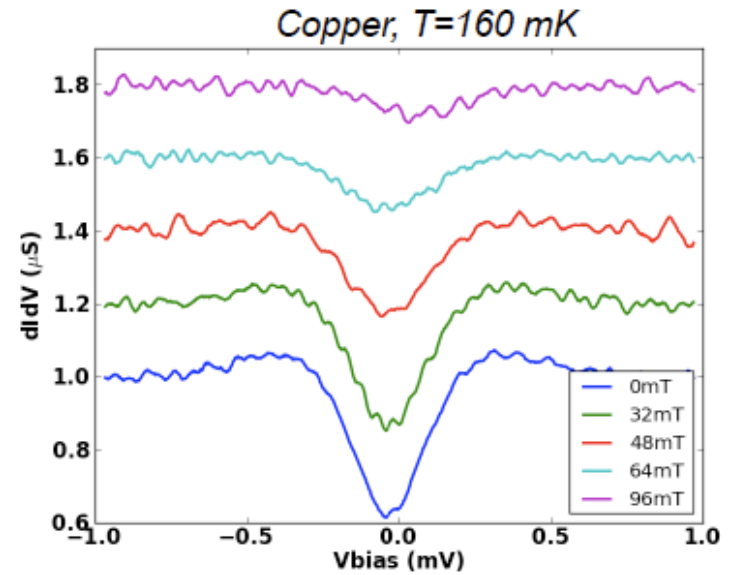
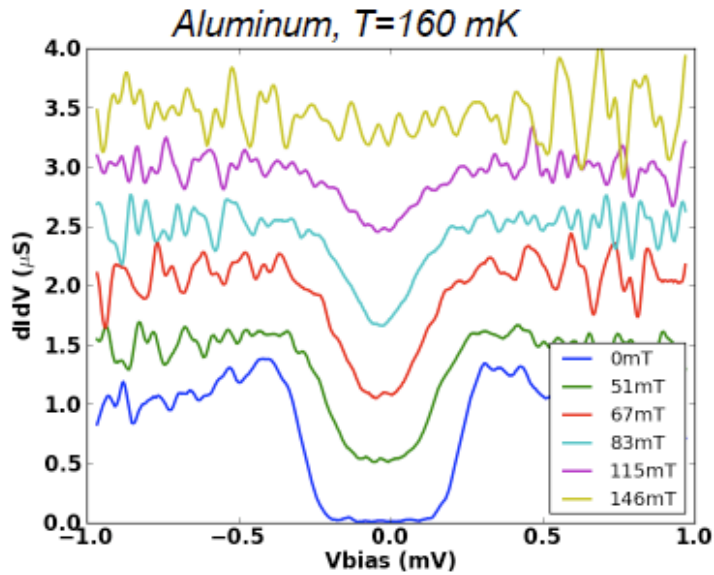
- Spatial dependence of proximity superconducting gap.
- Simultaneous transport measurement on S-N-S junction.
- Superconductivity lost simultaneously in normal island and aluminum leads : heating avalanche.

Local spectroscopy in superconducting devices

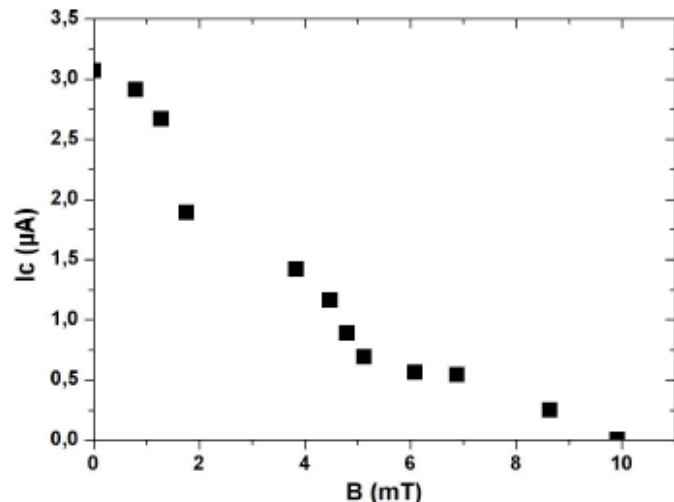


- Spatial dependence of proximity superconducting gap.
- Simultaneous transport measurement on S-N-S junction.
- Superconductivity lost simultaneously in normal island and aluminum leads : heating avalanche.

Local spectroscopy in superconducting devices



- Superconductivity in aluminum leads ($1\mu\text{m} \times 30\text{nm}$) suppressed at $\sim 140\text{ mT}$.
- Minigap signature in copper subsists up to $\sim 100\text{ mT}$.
- Junction critical current vanishes at 10 mT
 $(\leftrightarrow_0$ through $350 \times 600\text{ nm}^2$ junction)



Conclusions

- STM sensitive to both topography and density of states.
- Extremely fine and constraining measurements :
 $\partial z < 10\text{pm}$, $\partial I < 100\text{pA}$
challenging to combine with low temperatures
- A door to the nanoworld : access to local properties, local manipulation, study of mesoscopic devices.

Acknowledgments :

Hervé Courtois, Sylvain Martin, Julien Senzier, Nanofab

